DOI: 10.1021/ma902445u

Macromolecules
ARTICLE

Compartmentalization Effects on the Rate of Polymerization and the Degree of Control in ATRP Aqueous Dispersed Phase Polymerization

Mary E. Thomson and Michael F. Cunningham*

Department of Chemical Engineering, Queen's University, Kingston, Ontario, Canada K7L 3N6

Received November 4, 2009; Revised Manuscript Received January 28, 2010

ABSTRACT: Compartmentalization in atom transfer radical polymerization (ATRP) in an aqueous dispersed phase system has been investigated theoretically to understand the effects of particle size on the rate of polymerization and the degree of control on the livingness and polydispersity index (PDI) for the system *n*-butyl methacrylate/CuBr/EHA_6TREN. The simulations indicate that there exists a defined range of particle sizes where the rate of polymerization is higher than that of a bulk system and where PDI and frequency of termination remain below that of bulk polymerization. For this highly active catalyst system, the livingness of the chains is a function only of the particle size and is independent of the rate of reaction. Furthermore, simulations conducted with very low catalyst concentrations suggest that the rate of polymerization is dependent on the absolute amount of catalyst in the system rather than the steady-state Cu(I)/Cu(II) ratio that applies for bulk polymerization. At low catalyst concentrations, the rate of polymerization decreases, and the PDI increases with diminishing catalyst concentration, whereas the chain livingness is improved.

Introduction

Controlled/living polymerization has emerged as a powerful method for creating polymers with tailored molecular architectures under mild reaction conditions. However, this technology has not yet found widespread adoption for industrial production. One of the limitations is the difficulty associated with performing these polymerizations in aqueous dispersed systems such as emulsion or miniemulsion. Whereas dispersed phase polymerization is possible, the complexities of performing heterogeneous living polymerization are not yet fully understood.[1,2]

Recent experimental advances in ATRP miniemulsion polymerization have begun to make this polymerization technique more amenable to large-scale polymerization, especially AGET (activators generated by electron transfer) ATRP,[3−9] in which a reducing agent converts the less air-sensitive Cu(II) into Cu(I) in situ to begin the reaction. AGET ATRP also lends itself to lower catalyst concentrations. Simms and Cunningham have shown that reverse ATRP with the ligand EHA_6TREN can be performed in miniemulsion using a cationic surfactant,[10] which increases the stability of the emulsion system and allows higher temperature polymerization, and have also achieved very high molecular weight polymers with a fast reaction rate in a similar system.[11]

In bulk or solution ATRP, the steady-state rate of polymerization is controlled by the concentration of alkyl halide, $[P-X]$, and the ratio of Cu(I)/Cu(II) in the system, when termination reactions are considered to be negligible (eq 1). In this work, we discuss the first implications of low catalyst concentrations in aqueous dispersed phase polymerization. In bulk or solution polymerization, the basis for low catalyst ATRP is that the Cu(I)/Cu(II) ratio, rather than the absolute concentrations of either species, is rate determining. Therefore, low catalyst concentration ATRP systems, like ARGET (activators regenerated by electron transfer) and ICAR (Initiators for continuous activator regeneration), maintain a constant, high Cu(I)/Cu(II) ratio by regenerating Cu(I) from Cu(II) created through termination reactions either through the addition of a reducing agent or new radical generation respectively.[12]

$$R_p = k_p[M]\frac{k_{act}}{k_{deact}}[P-X]\frac{[Cu(I)]}{[Cu(II)]} \quad (1)$$

Conventional free radical emulsion polymerization exhibits a phenomenon called radical compartmentalization, whereby the propagating radicals present in different particles are unable to terminate mutually, thereby causing an increasing overall rate of reaction with diminishing particle size. In living/controlled polymerization, compartmentalization affects both the rate of termination and the rate of deactivation by the physical isolation of radicals and deactivating species inside separate particles; this was first observed through simulations for living polymerization controlled by reversible termination, namely, nitroxide-mediated polymerization (NMP)[13,14] and later for ATRP.[15] Compartmentalization has since been demonstrated experimentally in miniemulsion for both chemistries[16,17] with the observed rate of polymerization decreasing with decreasing particle size. In NMP, these compartmentalization effects appear to be dependent on the nitroxide type; whereas rate decreases were observed in miniemulsion using TEMPO,[16] with the higher activity and more hydrophilic nitroxide, SG1, compartmentalization effects have been found to reduce the rate of polymerization only to a small extent in microemulsion[18] and not at all in emulsion polymerization.[19] This was attributed to the SG1's slower deactivation rate and higher rate of exit from the particles into the aqueous phase. Mathematically, Charleux[20] has described NMP compartmentalization without the segregation of the nitroxide SG1. The lack of compartmentalization effects observed experimentally in these systems can be explained if the nitroxide is able to diffuse easily through the aqueous phase so fluctuations of the nitroxide concentration in each particle are negligible.

The compartmentalization effects of enhanced deactivation and radical segregation were first discussed by Zetterlund

*Corresponding author. E-mail: michael.cunningham@chee.queensu.ca.

 Published on Web 02/24/2010

and Okubo[14] in simulations of TEMPO-mediated styrene polymerization. The confined space effect leads to an increase in the rates of deactivation and termination inside the particle (compared to bulk polymerization) because the two molecules involved in the reactions are physically confined to a small reaction volume. Because of the confined space effect in ATRP, the rate of deactivation can mathematically be shown to be dependent on the volume of the particle as[15]

$$R_{\text{deact}} = \frac{k_{\text{deact}}}{(N_A V_p)^2} \sum_i \sum_j (i)(j) N_{i,j} \quad (2)$$

where $N_{i,j}$ is the fraction of particles containing i propagating radicals and j Cu(II) deactivator molecules, k_{deact} is the rate constant for deactivation, N_A is Avogadro's number, and V_p is the volume of the particle. Using a population balance approach, these studies by Zetterlund and Okubo[14] for NMP and by Kagawa et al.[15] for ATRP show that in the absence of new chain generation, the rate of polymerization first increases (because of radical segregation) and then diminishes (because of enhanced deactivation) with decreasing particle sizes.

Tobita[21−23] conducted Monte Carlo simulations to investigate compartmentalization effects in NMP. Whereas his results are consistent with the conclusions of Butte et al.[13] and Zetterlund and Okubo,[14] he also suggests that fluctuations in the number of deactivator molecules in the particles can lead to instances of higher radical concentrations and result in an increase in rate.[22] Zetterlund and Okubo attributed the same rate acceleration to radical segregation.[14]

Simulations of ATRP in dispersed systems have only been conducted for the ligand dNbpy,[15,24,25] which is a lower activity ligand and requires high catalyst concentrations and polymerization temperatures. Whereas dNbpy is soluble in monomer, the catalyst in the Cu(II) form does have a small but finite water solubility, which is known to be detrimental to maintaining control in ATRP miniemulsion polymerizations. Simulations examining the effect of Cu partitioning between the monomer and aqueous phases in a dNbpy ATRP system have been undertaken by Kagawa et al.[24] in the absence of compartmentalization effects. They concluded that the loss of deactivator, Cu(II), to the aqueous phase increased both the rate of polymerization and the polydispersity index (PDI). No previous published research has involved simulations using an active and highly hydrophobic ligand to study ATRP compartmentalization effects. We have simulated an ATRP system with the catalyst CuBr/EHA_6TREN.[10,11,17,26,27] This catalyst/ligand is a more suitable choice for examining compartmentalization, especially considering that compartmentalization effects have been observed experimentally with this catalyst system.[17] Compared with low activity ligand dNbpy, EHA_6TREN has negligible water solubility and a significantly higher K_{eq}, allowing polymerizations to be conducted at lower temperatures and with reduced catalyst concentrations. Whereas previous simulations[25] with dNbpy were limited to 1% conversion, we were able to run simulations with the high activity CuBr/EHA_6TREN catalyst up to 10% conversion.

Presented here is the first theoretical investigation of ATRP compartmentalization with a highly active catalyst/ligand system (CuBr/EHA_6TREN) and with low catalyst concentrations. We focus, in particular, on the PDI and livingness of the growing chains. There is a defined range of particle sizes where the rate of polymerization can be enhanced above that of bulk polymerization while maintaining excellent control, with an expected PDI and degree of termination below that of bulk polymerization. The implications of our findings to the possibility of using very low catalyst concentrations in ATRP-dispersed systems are discussed. These simulations differ significantly from previous ATRP simulations[15,25] in the selection of a high-activity catalyst/ligand system and in-depth examination of the effect of particle size on the PDI and the livingness of the system.

Model Development

Compartmentalized Model. The modified Smith−Ewart equations developed by Kagawa et al.[15] for ATRP were adapted and expanded to also track the moments of dormant and dead chains in the system, similar to the approach of Butte et al.[13] for NMP.

Both the propagating radicals and the deactivator, Cu(II), were considered to be compartmentalized species, as the contribution of individual molecules on the rates of reactions were accounted for, and these rates scale with the volume of the particle. The activating species, Cu(I), was considered to be uncompartmentalized because it is present in sufficient concentration in all particles that the fluctuations on a molecular basis inside individual particles will not be enough to significantly alter the rate.

The modified Smith-Ewart equations, including the compartmentalization of both radicals and Cu(II) are

$$\begin{aligned}\frac{dN_{i,j}}{dt} &= N_A V_p k_{act} \mu^{(0)} [\text{Cu(I)}](N_{i-1,j-1} - N_{i,j}) \\ &+ \frac{k_t}{N_A V_p}((i+2)(i+1)N_{i+2,j} - (i)(i-1)N_{i,j}) \\ &+ \frac{k_{\text{deact}}}{N_A V_p}((i+1)(j+1)N_{i+1,j+1} - (i)(j)N_{i,j}) \quad (3)\end{aligned}$$

$N_{i,j}$ is the fraction of particles with i radicals and j free $CuBr_2$/EHA_6TREN molecules, N_A is Avogadro's number, V_p is the volume of a particle, and $\mu^{(0)}$ is the zeroth order moment of the distribution of dormant chains (see below). The average number of radicals, Cu(II) and Cu(I) molecules per particle can be calculated by

$$\bar{n} = \sum_i \sum_j (i) N_{i,j} \quad (4)$$

$$\bar{n}_{\text{Cu(II)}} = \sum_i \sum_j (j) N_{i,j} \quad (5)$$

$$\bar{n}_{\text{Cu(I)}} = N_A V_p [\text{Cu(I)}] \quad (6)$$

Using the above averages directly makes it difficult to compare the rates of polymerization and concentrations of activating/deactivating species in particles of different sizes and systems with different concentrations of catalyst and initiator. Instead, the approach developed by Simms and Cunningham[17] is used where $\bar{n}_{\text{chain}}$ is defined as the average number of radicals per polymer chain in the system and $\bar{n}_{\text{Cu(II)chain}}$, similarly, is the average number of deactivating species per polymer chain. This method gives an absolute variation of polymerization rate on a chain-by-chain basis in the absence of other effects including that of catalyst and initiator concentration and also the number of particles in the system.

$$\bar{n}_{\text{chain}} = \frac{\bar{n}}{N_A V_p \mu_0^{(0)}} \quad (7)$$

$$\bar{n}_{\text{Cu(II)chain}} = \frac{\bar{n}_{\text{Cu(II)}}}{N_A V_p \mu_0^{(0)}} \quad (8)$$

To estimate the degree of polymerization (DP_n), the distribution of singly distinguished particles, $S_{i,j,m}$ is introduced, where $S_{i,j,m}$ is the fraction of particles containing i radicals, j Cu(II) molecules, and with a chain of length m.

$$\begin{aligned}\frac{dS_{i,j,m}}{dt} = {} & N_A V_p k_{act}[Cu(I)]\Big(\mu^{(0)} S_{i-1,j-1,m} + \\ & [P_m - X]N_{i-1,j-1} - \mu^{(0)} S_{i,j,m}\Big) \\ & + \frac{k_{deact}}{N_A V_p}\big((i)(j+1)S_{i+1,j+1,m} - (i)(j)S_{i,j,m}\big) \\ & + k_p[M]\big(S_{i,j,m-1} - S_{i,j,m}\big) \\ & + \frac{k_t}{N_A V_p}\big((i)(i+1)S_{i+2,j,m} - (i)(i-1)S_{i,j,m}\big) \end{aligned} \quad (9)$$

The PDI was estimated for the dormant chains only, as active chains were present in only extremely small concentrations. Likewise, dead chains will account for only a small fraction of total chains if the system is assumed to be highly living. The infinite set of equations (eq 9) is transformed into a finite set of equations by the method of moments, such that $\lambda_{i,j}^{(k)}$ is the k^{th} moment of growing chains present in each type of particle state, with i radicals and j Cu(II) molecules (eq 10). Therefore, the zeroth order moment, $\lambda_{i,j}^{(0)}$, is simply the overall number of active chains inside the particles of state i,j (eq 11).

$$\lambda_{i,j}^{(k)} = \sum_m m^k S_{i,j,m} \quad (10)$$

$$\lambda_{i,j}^{(0)} = (i)N_{i,j} \quad (11)$$

The mass balances for the uncompartmentalized species, such as monomer (eq 12), the zeroth through second moments of the dormant chains (eq 13), the concentration of activator, [Cu(I)] (eq 14), and the zeroth moment of the dead chains (eq 15) were also calculated.

$$\frac{d[M]}{dt} = \frac{k_p[M]}{N_A V_p}\bar{n} \quad (12)$$

$$\frac{d\mu^{(k)}}{dt} = -k_{act}[Cu(I)]\mu^{(k)} + \frac{k_{deact}}{(N_A V_p)^2}\sum_i\sum_j (j)\lambda_{i,j}^{(k)} \quad (13)$$

$$\frac{d[Cu(I)]}{dt} = \frac{k_{deact}}{(N_A V_p)^2}\sum_i\sum_j (j)\lambda_{i,j}^{(0)} - k_{act}[Cu(I)]\mu^{(0)} \quad (14)$$

$$\frac{d\zeta^{(0)}}{dt} = \frac{k_t}{(N_A V_p)^2}\sum_{i=2}\sum_j (i-1)\lambda_{i,j}^{(0)} \quad (15)$$

This system of differential equations was solved in Fortran by numerical integration with the solver DLSODI (backward Euler method) with a step size of 1 s. The differential equations were closed with a maximum of 6 radicals (i) and 75 Cu(II) molecules (j) per particle, well in excess of the ranges where compartmentalization effects are expected. Throughout all simulations, these boundary conditions were checked to ensure that these boundaries were not approached. Simulations investigating the livingness of the chains at 90% conversion were run with a maximum of 6 radicals and 200 Cu(II) molecules.

Bulk Polymerization Model. A bulk polymerization model was developed to estimate an $\bar{n}_{chain}$ equivalent, $\bar{n}_{chain}^{b}$, and PDI to compare directly with the dispersed phase polymerization system by applying the method of moments to the active chains of length m and the dormant chains of length m in a bulk polymerization system (eqs 16−19).

$$\begin{aligned}\frac{d[P_m\bullet]}{dt} = {} & k_{act}[P_m - X][Cu(I)] - k_{deact}[P_m\bullet][Cu(II)] - 2k_t \\ & \sum_{n=1}^{m-1}[P_n\bullet][P_{m-n}\bullet] + k_p[M][P_{m-1}\bullet] - k_p[M][P_m\bullet] \end{aligned} \quad (16)$$

$$\frac{d[Cu(I)]}{dt} = k_{deact}\sum_m [P_m\bullet][Cu(II)] - k_{act}[Cu(I)]\mu^{(0)} \quad (17)$$

$$\frac{d[P_m - X]}{dt} = -k_{act}[P_m - X][Cu(I)] + k_{deact}[P_m\bullet][Cu(II)] \quad (18)$$

$$\bar{n}_{chain}^{b} = \frac{\sum_m [P_m\bullet]}{\sum_m [P_m - X]} \quad (19)$$

Choice of Polymerization System. Compartmentalization in ATRP miniemulsion has been shown in a reverse ATRP system with *n*-butyl methacrylate (BMA) and using $CuBr_2$/EHA_6TREN.[17] Because compartmentalization effects on the rate of polymerization and the degree of control are similar regardless of the initiation system (forward ATRP, reverse ATRP, or AGET ATRP), a system of forward ATRP with BMA was chosen for these simulations for ease of calculation. (Also note that the use of a forward ATRP system is a simplification on an ARGET system, where all $CuBr_2$ is reduced to CuBr in situ at the beginning of the polymerization, independent of the generation of dormant chains). The ligand EHA_6TREN complexed to Cu(I) or Cu(II) demonstrates excellent monomer solubility and extreme hydrophobicity, and thus it is unlikely to partition to any appreciable degree into the aqueous phase, and phase transfer events can be neglected from the model with confidence. Other ligand systems used in miniemulsion, including BPMODA and dNbpy, possess some water solubility, especially for the $CuBr_2$/ligand species.

The rate coefficients of activation/deactivation for CuBr/EHA_6TREN have not been estimated in the literature, but approximate calculations from the apparent K_{ATRP} along with the published estimates for the structurally similar CuBr/BA_6TREN with EBiBr initiator (a 3° alkyl halide radical initiator with a structure similar to a BMA radical) were used in these simulations.[28] These calculated values are appropriate, best available estimates for the rate constants of CuBr/EHA_6TREN with BMA.

The simulations were conducted up to 10% conversion to minimize any conversion dependence on the rate coefficients. Chain length dependences of these constants were not taken into consideration. These simulations were conducted for varying particle sizes with a targeted degree of polymerization (at 100% conversion) between 100 and 5000 monomer units and with chain-to-catalyst ratios of 10:1, 2:1, and 1:1. The values of the parameters used are listed in Table 1.

Table 1. Values of the Parameters Used in Simulations

parameter	value
$[M]_0$	6.29 mol·L^{-1}
k_{act}	2.05 L·mol^{-1}·s^{-1} [28]
k_{deact}	3.9×10^7 L·mol^{-1}·s^{-1} [28]
k_p	1.24×10^3 L·mol^{-1}·s^{-1} [29]
k_t	1.03×10^7 L·mol^{-1}·s^{-1} [30]

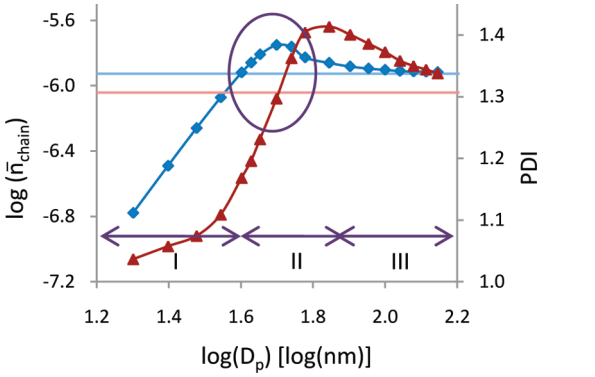

Figure 1. Effect of particle size on the reaction rate, as represented by $\bar{n}_{chain}$ (◆) and PDI (▲) at 10% conversion for the system with a targeted degree of polymerization of 500 and a 10:1 ratio of chains to Cu(I) at the start of the reaction. The solid lines represent the bulk equivalent $\bar{n}^b_{chain}$ and PDI.

Results and Discussion

Rate of Polymerization and the Degree of Control. Figure 1 shows the average number of radicals per chain (which is directly proportional to the rate of polymerization) and the PDI at 10% conversion over a range of particle sizes for the BMA/CuBr/EHA$_6$TREN system simulated at 70 °C for a targeted degree of polymerization (DP_n) of 500 and an initiator/Cu(I) ratio of 10:1 (one Cu molecule mediates ten chains). The rate of polymerization increases with increasing particle size to a maximum and levels out to the rate in an equivalent bulk system. This type of correlation is expected based on previous ATRP simulations,[15,25] but the relationship of PDI with particle size has not yet been discussed because previous models were unable to estimate this. The PDI also increases, goes through a maximum, and subsequently levels out to the same PDI as an equivalent bulk system with increasing particle size, but the maximum occurs at an offset with respect to the maximum of the rate of polymerization. In the system presented here (Figure 1), the time required to reach 10% conversion at 45 nm is 15 times faster than that for the particle size of 20 nm. Similarly, in a system with a target DP_n of 5000 and a chain/catalyst ratio of 10:1, the time to reach 10% conversion in a 120 nm particle is four times as fast as a particle of 60 nm (in the enhanced deactivation region) while also being 1.3 times faster than a 240 nm particle (in the approach to bulk region).

In an effort to aid the comparison of these living/controlled dispersed phase polymerization systems to the better known conventional systems, $\bar{n}$, not just $\bar{n}_{chain}$, was also evaluated. Whereas in conventional systems (for the simplified case of termination as the main chain stopping event), $\bar{n}$ remains ~0.5 regardless of the particle size. The situation is much more complicated in controlled polymerization because $\bar{n}$ is dependent not only on the size of the particles but also the total concentration of chains in the system. This difference arises because deactivation, not termination, becomes the dominant chain stopping effect. Over a range of particle sizes (keeping a constant targeted degree of polymerization), $\bar{n}$ increases with increasing particle size (or with a decrease in the total number of particles). For the simulations discussed in Figures 1 and 2, the absolute $\bar{n}$ is much lower than in conventional systems and varies between 10^{-7} and 10^{-6} over the range of particle sizes discussed.

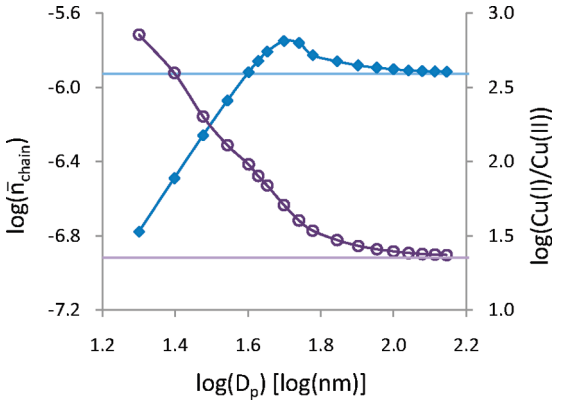

Figure 2. Effect of particle size on the reaction rate, as represented by $\bar{n}_{chain}$ (◆) and Cu(I)/Cu(II) (○) at 10% conversion for the system with a targeted degree of polymerization of 500 and a 10:1 ratio of chains to Cu(I) at the start of the reaction. The solid lines represent the bulk equivalent $\bar{n}^b_{chain}$ and Cu(I)/Cu(II).

The rate of polymerization (as indicated by $\bar{n}_{chain}$) and PDI change dramatically with particle size and can be considered to be three different regions, as explained below.

Region I: Enhanced Deactivation. At very small particle sizes, the rate of reaction and the PDI are significantly lower than bulk and decrease with diminishing particle size. This can be attributed to the effect of enhanced deactivation described by Kagawa et al.[15] In this regime, the concentration of radicals in the system is proportional to the volume of the particle (or [P•] is proportional to d^3), and termination is negligible. The slope of the log−log plot (Figures 1 and 2) of $\bar{n}_{chain}$ versus particle size is linear with a slope of 3. In qualitative terms, this means that following a single activation, the concentration of deactivator in the system is greater (based on $\bar{n}_{Cu(II)}/N_A V_p$) in smaller particles, causing the chain to deactivate more quickly. In terms of reaction rate, this leads to a slower polymerization, assuming that activation occurs at a consistent rate regardless of the particle size. This is always the case, regardless of the particle size region, for nitroxide-mediated polymerization, where activation is controlled by a thermal process; it is also the case in region I for ATRP when the activator Cu(I) is considered to be uncompartmentalized and termination is negligible, and thus the Cu(I) local concentration is not affected by the change of a single molecule from Cu(I) to Cu(II). In this region, the PDI of the living chains is also lower because fewer units are added per activation cycle with diminishing particle size, and more cycles are required to reach the same conversion. This will be discussed later in further detail.

Region II: Acceleration Window. The increase in the rate of reaction above that predicted in an equivalent bulk system was described by Kagawa et al.[15] in terms of radical segregation (because radicals in different particles are unable to mutually terminate) and in NMP by Tobita[22] as the fluctuation effect, where the local concentration of deactivator in the particles changes with every activation/deactivation reaction. Our results indicate that the acceleration window observed in an ATRP system can be attributed to the nonestablishment of a Cu(I)/Cu(II) steady state ratio, as is observed in bulk polymerization (eq 1), owing to fewer instances of termination early in the polymerization, which

is the result of both enhanced deactivation and radical segregation. Kagawa et al.[15] reported that with moderate particle sizes, lower numbers of deactivator molecules in the particles reduced the degree of control by increasing the number of units added per activation. However, in our simulations, the effect of a lower number of deactivating molecules can also be seen as an increase in the frequency of activation events by the presence of a larger concentration of activator and an overall faster rate of polymerization.

Figures 2 shows the Cu(I)/Cu(II) ratio and the variation in the average number of radicals per chain with particle size for the same system with a target DP_n of 500 and an initiator/Cu(I) ratio of 10:1. The steady-state Cu(I)/Cu(II) equilibrium ratio, which is a characteristic of bulk and solution ATRP, is not achieved in the acceleration window because very little termination occurs in the particles (because of the enhanced deactivation allowing fewer active radicals as well as radical compartmentalization preventing the mutual termination of radicals present in different particles). Therefore, at small particle sizes, the system will always possess a concentration of activator, Cu(I), which is larger than in bulk systems. This leads to more frequent activation cycles than in bulk polymerization, increasing the $\overline{n}_{chain}$. Whereas Cu(II) compartmentalization serves as the major compartmentalization effect in these systems, lowering $\overline{n}_{chain}$ with diminishing particle sizes, the secondary and contrary effect of more frequent activation cycles, owing to lower termination and leading to an increase in $\overline{n}_{chain}$ with diminishing particle sizes (described above), is also at play. Without the secondary enhanced activation effect, the $\overline{n}_{chain}$ and PDI trends with particle size would overlap; it is this secondary effect arising from the minimization of termination and the increase in the absolute concentration of Cu(I) inside the particles that allows a region of particle sizes where the rate of reaction can be above that in an equivalent bulk system while still maintaining a PDI below that in bulk.

Region III: Approach to a Bulk System. At larger particle sizes, the anticipated $\overline{n}_{chain}$ approaches that of a bulk polymerization (Figure 1) because more radicals are present at any time, with consequently less influence of enhanced deactivation and increased termination. The Cu(I)/Cu(II) ratio approaches that of the bulk system (Figure 2).

Regions for the PDI. According to the method developed by Goto and Fukuda[31] for bulk systems, the PDI of the living chains is influenced by both the number of units added per activation as well as the number of activation cycles to reach a given conversion.

$$\begin{aligned}\text{no. units} &= \frac{\text{propagation}}{\text{deactivation}} \\ &= \frac{k_p[M][P\bullet]}{k_{deact}[Cu(II)][P\bullet]} \\ &= \frac{k_p[M]\dfrac{\sum_i (i)N_{i,j}}{N_A V_p}}{k_{deact}\dfrac{\sum_i \sum_j (i)(j)N_{i,j}}{(N_A V_p)^2}} \\ &= \frac{k_p[M]N_A V_p \overline{n}}{k_{deact}\sum_i \sum_j (i)(j)N_{i,j}} \propto d^3 \end{aligned} \quad (20)$$

The multiple influences of compartmentalization on the PDI in the dispersed phase can be broken down into several different effects. As previously discussed, the number of units added per activation is influenced by enhanced deactivation in smaller particle sizes. The number of units added is a function of the ratio of the rate of propagation with respect to the rate of deactivation and can be transformed to a proportionality (eq 20) with respect to the particle diameter cubed, d^3, through the application of the eqs 2 and 4 along with the understanding that $[P\bullet]$ can be obtained by $\overline{n}/N_A V_p$. However the frequency of the activation cycles is similarly influenced by the concentration of Cu(I), which is higher in smaller particles. Finally, the number of activations required to reach a given conversion is different for each particle size. Therefore, the contrasting effects of enhanced deactivation and the concentration of Cu(I) in the calculation of the PDI are influenced in a different manner than the rate of polymerization. This leads to a general trend of increasing PDI with particle size in region I of enhanced deactivation (because of the number of units added per activation increasing with particle size). At moderate particle sizes, the PDI passes through a range of particle sizes where the simulated PDIs of the living chains are greater than that in bulk (attributed to the lower instances of termination in the dispersed phase, which lead to a lower rate of deactivation and the addition of more units per cycle than in the bulk system). Finally the PDI decreases with increasing particle size in region III owing to irreversible termination and the buildup of Cu(II) in the system, pushing the equilibrium to favor the dormant chains (Figure 1). The window where the PDI is greater in the emulsion system than in bulk occurs at larger particle sizes than the acceleration window for the rate of polymerization. Therefore, there exists a range of particle sizes where the rate of polymerization is higher than that of bulk polymerization but where we can preserve a high degree of control over the PDI and livingness, which is greater than an equivalent bulk system.

Effect of the Targeted Degree of Polymerization. In ATRP systems, modifying the targeted degree of polymerization is simply a matter of modifying the alkyl halide initiator concentration. Because the polymerization kinetics are often thought in terms of the number of chains each Cu(I) molecule can mediate, the overall concentration of Cu(I) is similarly modified with the target DP_n. This section presents the results of simulations for the system of BMA/CuBr/EHA_6TREN with a alkyl halide initiator/catalyst ratio of 2:1 and targeted degrees of polymerization ranging from 100 to 5000, or targeted molecular weights (M_n) of 14 200 to 710 000 g/mol.

As expected, the degree of livingness of the polymer chains increases with diminishing particle size (Figure 3c) and is attributed to the suppression of termination due to the compartmentalization of the radicals. It should be noted that the degree of termination never exceeds that expected in the bulk system, indicating that although there is a particle size range where the rate of polymerization exceeds that in bulk (Figure 4a), the livingness of the system will not be adversely affected by operating in that range.

At a given particle size, log(Cu(I)/Cu(II)) increases when the targeted DP_n is increased (or the concentration of initiator is decreased) (Figure 4b). This trend is contrary to that predicted by the persistent radical effect[32] in bulk polymerization. The persistent radical effect predicts that when the concentration of initiator is decreased, the concentration of deactivator (Cu(II)) will increase to maintain an equilibrium through the mutual termination of chains. However, in the dispersed phase, where termination is suppressed through compartmentalization, the persistent radical effect is similarly suppressed. Because the concentration of Cu(II) does not rise considerably in systems with lower concentrations of initiator, and termination is further

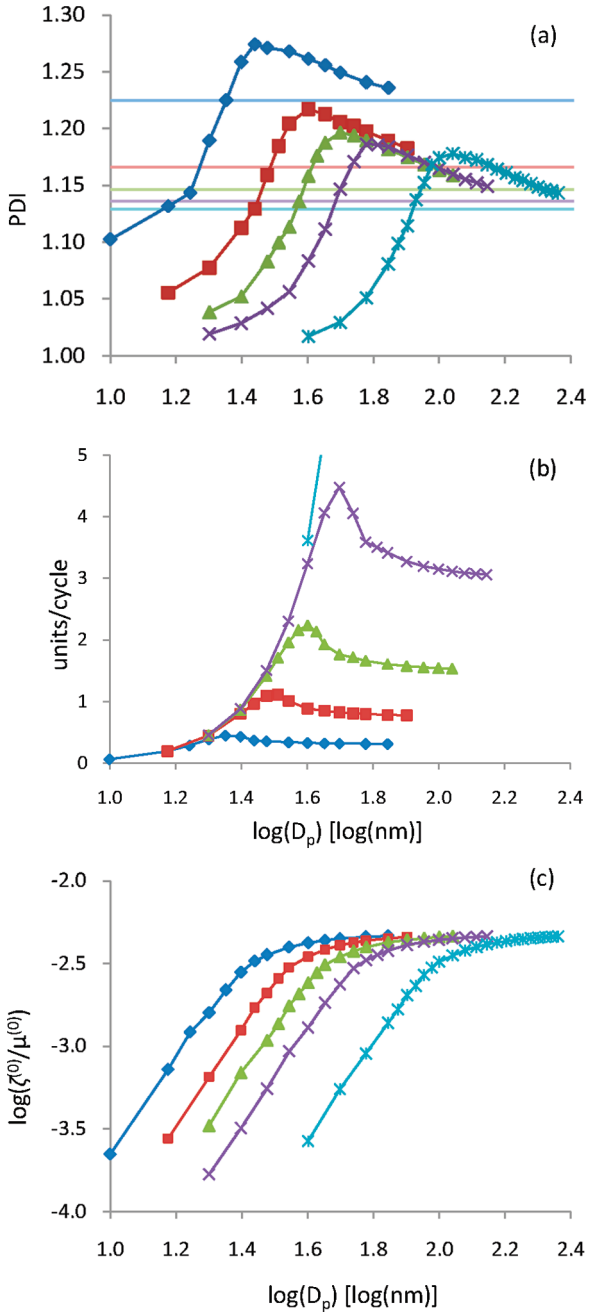

Figure 3. Simulations conducted up to 10% conversion with an initiator/Cu(I) ratio of 2:1 to investigate the effect of (a) the PDI, (b) the number of units added per activation cycle, and (c) the ratio of dead/dormant chains at 10% conversion with respect to particle size for systems with target degrees of polymerization (at 100% conversion) of 100 (◆), 250 (■), 500 (▲), 1000 (×), and 5000 (∗).

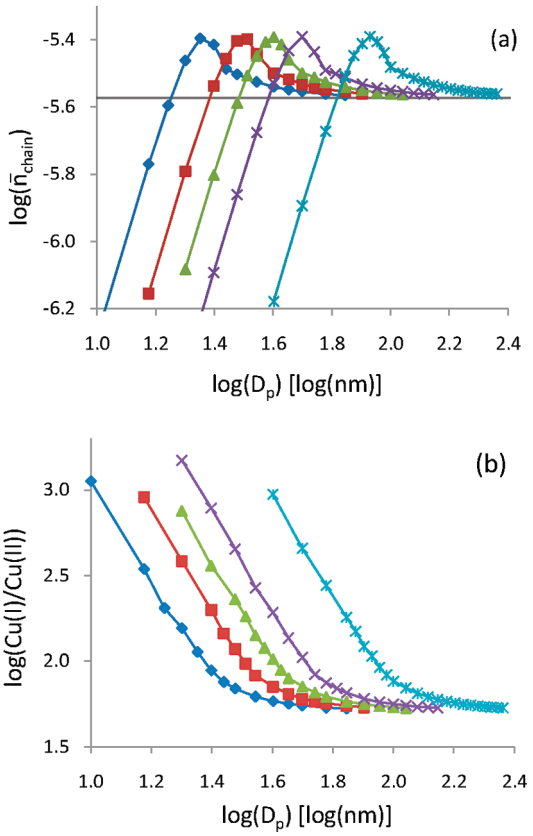

Figure 4. Simulations conducted up to 10% conversion with an initiator/Cu(I) ratio of 2:1 to investigate the effect of (a) the rate of polymerization as represented by the average number of radicals per chain, $\bar{n}_{chain}$ and (b) the ratio of Cu(I)/Cu(II) with respect to particle size for systems with target degrees of polymerization (at 100% conversion) of 100 (◆), 250 (■), 500 (▲), 1000 (×), and 5000 (∗).

suppressed in these particles (Figure 3c), the ratio of Cu(I)/Cu(II) will be greater in systems with higher targeted DP_n values.

There is a similar argument concerning the higher PDIs obtained in systems with lower initiator concentrations (or lower target DP_n values) specifically in the approach to bulk region (Figure 3a). This is contrary to what is expected in a bulk polymerization. Because the PDI is dependent on a ratio of the concentration of chains with respect to the concentration of Cu(II) in the system,[31] the persistent radical effect predicts that the PDI would be uniformly higher for the systems with higher initiator concentrations. However, the lower instances of termination in systems with higher target DP_n values lead to a lower-than-predicted concentration of Cu(II) present in the particles, yielding higher PDIs at higher target DP_n values. The PDI trends in the other regions (enhanced deactivation and the acceleration window) are discussed below.

In simulations up to 10% conversion in compartmentalized systems, the livingness of the chains remains above 98% for all of the conditions simulated, including different targeted DP_n values and with different concentrations of catalyst. This is a common phenomenon in previous ATRP[25] and NMP[14] population balance simulations. However, this livingness is likely dependent on the activity of the nitroxide or ATRP catalyst. When the simulations here are run to a higher conversion, for example, in the system of 100 nm particles with a targeted DP_n of 1000 and a 1:1 chain/catalyst ratio, the livingness of the system at 90% conversion is calculated to be 94%. Simulations to high conversion are quite computationally intensive because the number of free Cu(II) molecules accounted (j) must be increased from 75 to 200 to maintain a closed system of equations.

While removing the effect of the total concentration of chains in the system, through the use of $\bar{n}_{chain}$ rather than $\bar{n}$ or [P•] directly, the rate of monomer addition per chain in the system levels out to the same rate for larger particle sizes and for the bulk system (Figure 4a), however the PDI of these chains does not (Figure 3a). The PDI is affected by the total number of activations required to reach 10% conversion and also the number of units added in each of these activations. In general, the PDI diminishes with increasing particle size because of a balance between the number of activations (DP_n 5000 experiences the most, generally lowering the PDI) and the number of units added (at 10% conversion, DP_n 5000

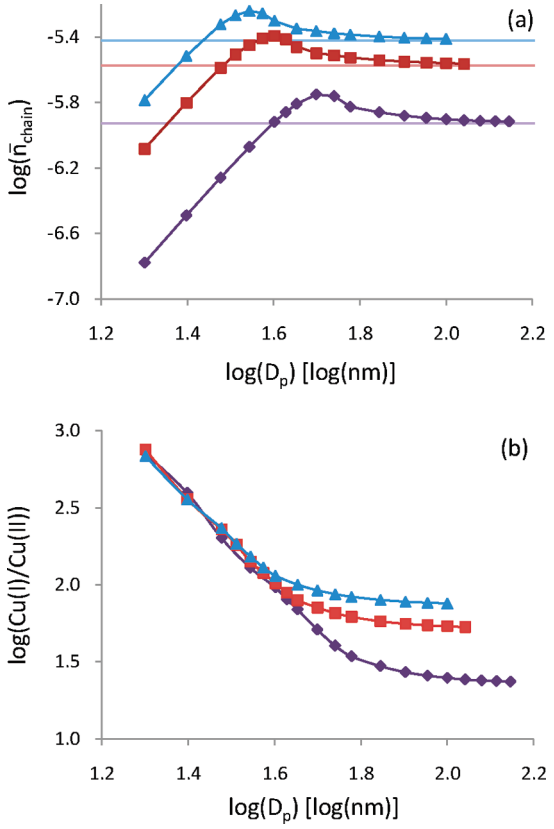

Figure 5. Simulations conducted up to 10% conversion with a targeted degree of polymerization of 500 (at 100% conversion) to investigate the effect of (a) the rate of polymerization as represented by the average number of radicals per chain, $\bar{n}_{chain}$, and the bulk system, $\bar{n}^{b}_{chain}$ (solid lines), and (b) the ratio of Cu(I)/Cu(II) with respect to particle size for systems with initiator/Cu(I) ratios of 10:1 (◆), 2:1 (■), and 1:1 (▲).

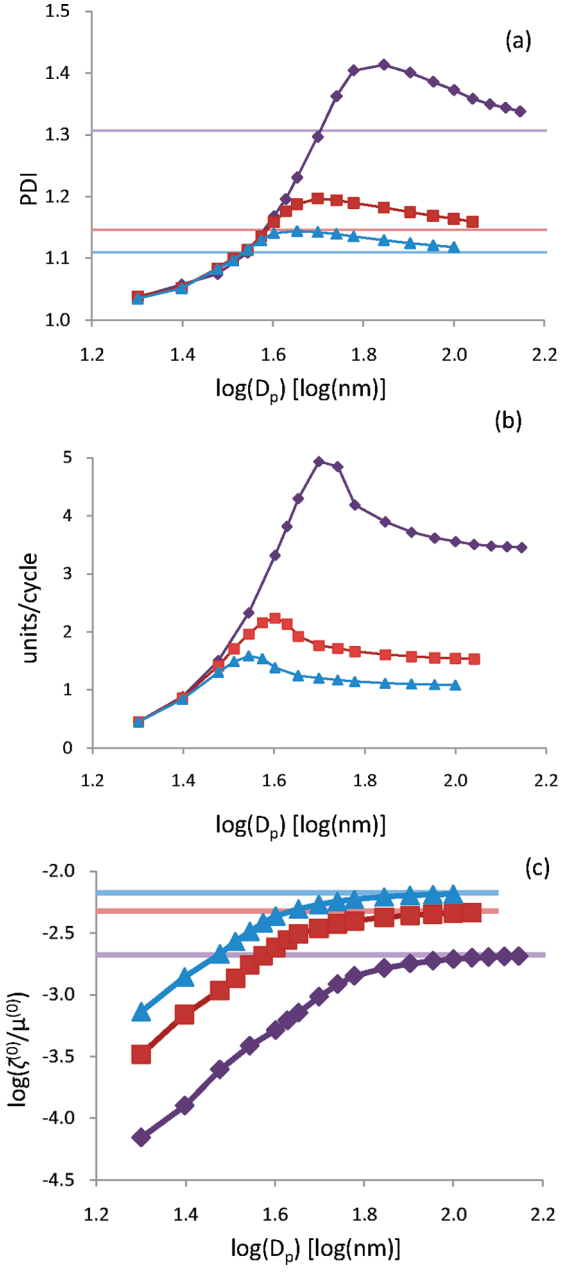

Figure 6. Simulations conducted up to 10% conversion with a targeted degree of polymerization of 500 (at 100% conversion) to investigate the effect of (a) the PDI, (b) the number of units added per activation cycle, and (c) the ratio of dead/dormant chains at 10% conversion with respect to particle size for systems with initiator/Cu(I) ratios of 10:1 (◆), 2:1 (■), and 1:1 (▲).

adds far more units per activation, which in general tends to increase the PDI). Under the conditions simulated here (Figure 3a,b), the number of activations plays a far more important role in determining the overall PDI of the dormant chains than does the number of units added per activation.

Effect of the Catalyst Concentration. With considerable interest in achieving lower catalyst concentrations in solution and bulk ATRP, preliminary investigations into the reduction of catalyst concentration in aqueous dispersed phase polymerization were undertaken. Unlike ARGET and ICAR chemistries, no Cu(I) regeneration mechanisms are included in the simulations, but it will become apparent that the nonestablishment of a steady state Cu(I)/Cu(II) ratio and diminishing instances of termination (Figures 5b and 6c) allows the total catalyst concentration to be reduced and polymerization to continue without a large buildup of Cu(II) occurring and suppressing the polymerization rate.

Simulations were conducted for the system with a targeted degree of polymerization of 500 and varying initiator/catalyst ratios of 10:1, 2:1, and 1:1 (Figures 5 and 6). These are the first simulation results that detail the effects of diminishing catalyst concentration in dispersed phase ATRP polymerization, and some unique features are revealed. First, in the region I (enhanced deactivation) of Figure 5, the Cu(I)/Cu(II) ratio remains the same for all three catalyst concentrations, however the rate of polymerization ($\bar{n}_{chain}$), which takes into account the effect of the initiator concentration, diminishes with diminishing catalyst concentration. This result is contrary to the commonly accepted rate expression for solution ATRP (eq 1) in that the rate in the dispersed phase is dependent on the absolute concentration of catalyst. However, in bulk, only the ratio of Cu(I)/Cu(II), which remains unchanged in these simulations, should affect the rate. Therefore, in aqueous dispersed phase polymerizations, the rate of polymerization is dependent on the total concentration of activator, Cu(I), present in the system when termination is suppressed, and a steady-state Cu(I)/Cu(II) ratio is not achieved in the early stages of the polymerization, as is the case for bulk and solution polymerization. In regions II and III, it becomes clear that the steady-state Cu(I)/Cu(II) ratio achieves different values and $\bar{n}_{chain}$ also reaches different steady state (and bulk) rates with diminishing catalyst concentration.

The PDI is greatly influenced by the total concentration of deactivating species in the system, Cu(II), because larger

concentrations of deactivator lead to the addition of fewer units per activation, and thus more activations are required to reach a given conversion. In these simulations, which all possess the same concentration of initiator but varying concentrations of catalyst, the system with the lowest catalyst concentration (10:1 initiator/catalyst ratio) shows the lowest Cu(I)/Cu(II) ratio (Figure 5b) but possesses the lowest overall concentration of Cu(II). Therefore, the PDI (Figure 6a) and the number of units added per activation event (Figure 6b) are significantly larger than those for the other systems. Therefore, targeting a lower catalyst concentration not only leads to diminished rates of polymerization but also results in a significantly higher PDI. It should be noted, however, that the livingness of the system is higher in systems possessing a lower concentration of catalyst because the ratio of dead chains/dormant chains is lower for all particle sizes (Figure 6c).

On the basis of these simulations, a discussion of the application to low catalyst systems, such as ARGET and ICAR, is warranted. In the ARGET system, regeneration of the Cu(I) from Cu(II) may lead to increasing the Cu(I)/Cu(II) ratio for larger particle sizes (especially in region III) but will have no effect in region I, where termination is negligible and Cu(I) regeneration is not necessary. In this region, PDI will increase, and the rate will diminish as the concentration of Cu is lowered, but the chains will retain a greater livingness. In regions I and II, ICAR chemistry and the addition of a secondary radical source may cause further irreversible terminations. In small particles, when a second radical enters into a particle that is already containing an active radical, termination is instantaneous (a zero-one system) and could lead to the buildup of Cu(II) and also decrease the livingness of the system. In region III, ICAR may be of use to generate new chains because termination is not instantaneous between radicals and there is a larger buildup of Cu(II) at any given conversion. However, in this region, ARGET is less likely to diminishing the livingness of the system.

Conclusions

Compartmentalization effects can influence the rate of polymerization, the degree of control of the PDI, and the livingness of the polymer formed in aqueous dispersed phase ATRP polymerizations. For the highly active catalyst CuBr/EHA_6TREN, it was found that for small particle sizes, both the rate of polymerization and the number of units added per activation decreased proportionally to the volume of the particles, attributed to the confined space effect influencing the rate of deactivation of the chains. It was also found that there exists a window of particle sizes where the rate of polymerization is higher than that of a bulk system but where the PDI and the degree of termination remain below that of bulk, indicating an optimal region of particle sizes. Whereas the rate of polymerization is directly controlled by an equilibrium ratio of Cu(I)/Cu(II) for bulk ATRP systems, this is not true for the compartmentalized system, where the rate is instead controlled by enhanced deactivation and also the relative concentration of Cu(I) and Cu(II), which are dependent on the size of the particles.

When changing the concentration of initiator in the system to target different DP_n values, the range of particle sizes where the rate of polymerization exceeds that of bulk is shifted to lower particle sizes with increased initiator concentration, but as the effect of enhanced deactivation is minimized (at larger particle sizes), the rate at which monomer units are added to a single polymer chain in the system does not change with initiator concentration, provided that the initiator/catalyst concentration remains constant. However, the number of activations required to reach a given conversion has a greater effect on the final PDI than does the number of units added per activation because systems with the lowest initiator concentration achieve the lowest PDI for all particle sizes, even while adding the most monomer units per activation.

In this ATRP system, several important points concerning ATRP with low catalyst concentrations in the aqueous dispersed phase are highlighted. First, lower catalyst concentrations lead to slower polymerization rates because the frequency of activation events is lower, whereas the PDI and the number of units added per chain are higher. However, polymerizations conducted under these conditions do possess a greater livingness. The application of ARGET or ICAR chemistries will not improve the rate of polymerization in the smallest particles, and the generation of new radicals in the ICAR chemistry may have a detrimental effect on the livingness of the system.

Acknowledgment. We thank Dr. A. Butté from ETH (Zurich) for many helpful discussions on compartmentalization and the Natural Sciences and Engineering Research Council of Canada (NSERC) for financial support.

References and Notes

(1) Cunningham, M. F. *Prog. Polym. Sci.* **2008**, *33*, 365–398.
(2) Zetterlund, P. B.; Kagawa, Y.; Okubo, M. *Chem. Rev.* **2008**, *108*, 3747–3794.
(3) Min, K.; Gao, H.; Matyjaszewski, K. *J. Am. Chem. Soc.* **2005**, *127*, 3825–3830.
(4) Min, K.; Jakubowski, W.; Matyjaszewski, K. *Macromol. Rapid Commun.* **2006**, *27*, 982–982.
(5) Stoffelbach, F.; Belardi, B.; Santos, J. M. R. C. A.; Tessier, L.; Matyjaszewski, K.; Charleux, B. *Macromolecules* **2007**, *40*, 8813–8816.
(6) Min, K.; Yu, S.; Lee, H.; Mueller, L.; Sheiko, S. S.; Matyjaszewski, K. *Macromolecules* **2007**, *40*, 6557–6563.
(7) Stoffelbach, F.; Griffete, N.; Bui, C.; Charleux, B. *Chem. Commun.* **2008**, 4807–4809.
(8) Dong, H.; Mantha, V.; Matyjaszewski, K. *Chem. Mater.* **2009**, *21*, 3965–3972.
(9) Li, W.; Matyjaszewski, K.; Albrecht, K.; Moller, M. *Macromolecules* **2009**, *21*, 8228–8233.
(10) Simms, R. W.; Cunningham, M. F. *J. Polym. Sci., Part A: Polym. Chem.* **2006**, *44*, 1628–1634.
(11) Simms, R. W.; Cunningham, M. F. *Macromolecules* **2007**, *40*, 860–866.
(12) Braunecker, W. A.; Matyjaszewski, K. *Prog. Polym. Sci.* **2007**, *32*, 93–146.
(13) Butte, A.; Storti, G.; Morbidelli, M. *DECHEMA Monogr.* **1998**, *134*, 497–507.
(14) Zetterlund, P. B.; Okubo, M. *Macromolecules* **2006**, *39*, 8959–8967.
(15) Kagawa, Y.; Zetterlund, P. B.; Minami, H.; Okubo, M. *Macromol. Theory Simul.* **2006**, *15*, 608–613.
(16) Maehata, H.; Buragina, C.; Cunningham, M.; Keoshkerian, B. *Macromolecules* **2007**, *40*, 7126–7131.
(17) Simms, R. W.; Cunningham, M. F. *Macromolecules* **2008**, *41*, 5148–5155.
(18) Zetterlund, P. B.; Wakamatsu, J.; Okubo, M. *Macromolecules* **2009**, *42*, 6944–6952.
(19) Delaittre, G.; Charleux, B. *Macromolecules* **2008**, *41*, 2361–2367.
(20) Charleux, B. *Macromolecules* **2000**, *33*, 5358–5365.
(21) Tobita, H.; Yanase, F. *Macromol. Theory Simul.* **2007**, *16*, 476–488.
(22) Tobita, H. *Macromol. Theory Simul.* **2007**, *16*, 810–823.
(23) Tobita, H. *Macromol. Symp.* **2008**, *261*, 36–45.
(24) Kagawa, Y.; Zetterlund, P. B.; Minami, H.; Okubo, M. *Macromolecules* **2007**, *40*, 3062–3069.
(25) Zetterlund, P. B.; Kagawa, Y.; Okubo, M. *Macromolecules* **2009**, *42*, 2488–2496.
(26) Li, M.; Matyjaszewski, K. *Macromolecules* **2003**, *36*, 6028–6035.
(27) Li, M.; Min, K.; Matyjaszewski, K. *Macromolecules* **2004**, *37*, 2106–2112.
(28) Tang, W.; Kwak, Y.; Braunecker, W.; Tsarevsky, N. V.; Coote, M. L.; Matyjaszewski, K. *J. Am. Chem. Soc.* **2008**, *130*, 10702–10713.
(29) Beuermann, S.; Buback, M.; Davis, T. P.; Gilbert, R. G.; Hutchinson, R. A.; Kajiwara, A.; Klumperman, B.; Russell, G. T. *Macromol. Chem. Phys.* **2000**, *201*, 1355–1364.
(30) Buback, M.; Junkers, T. *Macromol. Chem. Phys.* **2006**, *207*, 1640–1650.
(31) Goto, A.; Fukuda, T. *Prog. Polym. Sci.* **2004**, *29*, 329–385.
(32) Fischer, H. *Chem. Rev.* **2001**, *101*, 3581–3610.